Mon. Not. R. astr. Soc. (1981) **197**, 995–1019

The evolution of flows of stellar mass loss in active galaxies

J. MacDonald and M. E. Bailey *Astronomy Centre, University of Sussex, Falmer, Brighton, Sussex BN1 9QH*

Received 1981 April 2; in original form 1981 February 11

Summary. Gas flows in elliptical galaxies fuelled by stellar mass loss have been calculated numerically for three fiducial epochs using both King and de Vaucouleurs models of NGC 3379. Our results show that supernova heating is unable to prevent the inflow of stellar mass loss for a large proportion of the lifetime of most giant elliptical galaxies, irrespective of their detailed structure. At the present epoch, stellar mass loss flows inwards in those elliptical galaxies with mean line-of-sight velocity dispersion $\bar{\sigma} > \sigma_{tr} \simeq 300\,\mathrm{km\,s^{-1}}$. At earlier epochs the transition velocity dispersion σ_{tr}, dividing galaxies with inflow from those with total winds ($\bar{\sigma} < \sigma_{tr}$), is smaller and allows less massive ellipticals to retain their stellar mass loss. Evolution in σ_{tr} is caused principally by evolution in the stellar mass loss rate. Because of the steepness of the galaxy mass function at the relevant masses, this leads to a rapid increase with redshift of the comoving density of active galaxies. Our model explains the association of nuclear activity with giant elliptical galaxies and predicts rapid comoving density evolution as observed. This work demonstrates the importance of considering the fate of stellar mass loss in elliptical galaxies.

1 Introduction

An important problem of galactic evolution is the fate of stellar mass loss in elliptical galaxies. Observations give little evidence for appreciable amounts of gas or significant rates of star formation in most of these systems (Faber & Gallagher 1976). The absence of interstellar material can be understood if there is an effective gas removal mechanism, e.g. a supernova-driven galactic wind (Mathews & Baker 1971) or ram-pressure stripping (Gisler 1976). However, some elliptical galaxies do contain gas (Minkowski & Osterbrock 1959; Osterbrock 1960; Gallagher *et al.* 1977; Fosbury *et al.* 1978). Also a significant fraction of massive ellipticals show various indications of energetic nuclear activity (Colla *et al.* 1975; Condon & Dressel 1978). This suggests that under some circumstances stellar mass loss does not flow out of the galaxy but accumulates and flows inwards to the centre (Mathews & Baker 1971; Bregman 1978; Bailey 1980).

This paper considers the problem of gas flow in elliptical galaxies from an evolutionary standpoint, concentrating particularly on the effects of the higher stellar mass loss rates

expected at earlier epochs. The results of a number of detailed numerical calculations are presented for two types of galaxy model. Because of uncertainty concerning the correct surface brightness profiles of elliptical galaxies (King 1978; Schweizer 1979) we consider models of galaxies obeying the empirical $r^{1/4}$ law (de Vaucouleurs 1959) and also models constructed according to the theory of King (1966).

Our calculations differ from those of Mathews & Baker (1971) in that we use somewhat lower values of the specific mass loss rates for both stars and supernovae in accord with more recent observational data. Also our galaxy models are consistent in the sense that the velocity dispersion profile is calculated from the stellar density distribution.

The details of our model for the wind are given in Section 2. A simple picture of how elliptical galaxies might evolve due to stellar mass loss is discussed in Section 3. In Section 4 we give some approximate analytic results on when inflow may occur. The results of the numerical calculations are presented in detail in Section 5. Discussion of the relevance of galactic winds/inflows to the evolution of active galaxies and their number density is given in Section 6. Our conclusions are summarized in Section 7.

2 The galactic wind model

2.1 BASIC EQUATIONS

We restrict ourselves to spherically symmetric galaxies in which the stellar density, ρ_*, the gravitational force due to stars, g_*, and the stellar velocity dispersion, σ_*, are functions only of radius. Stars are assumed to lose mass by winds and/or ejection of planetary nebulae at a rate per unit volume of $\alpha_*\rho_*$. At a particular epoch the specific mass loss rate for stars, α_*, is assumed constant and uniform. The stellar mass loss is assumed to mix rapidly with the galactic wind and, because of the random motion of the stars, to put energy into the wind at rate $\alpha_*\rho_*\ \frac{1}{2}\sigma_*^2$ per unit volume. The major source of energy for driving a galactic wind, however, is supernovae which are assumed to inject mass and energy into the wind at rate $\alpha_{SN}\rho_*$ and $\alpha_{SN}E_{SN}\rho_*$ per unit volume respectively. The specific mass loss rate for supernovae, α_{SN}, and the energy per unit mass of supernovae ejecta, E_{SN}, are also assumed constant and uniform. The reasons for this assumption are given in the next section.

The Eulerian time-dependent flow equations for the wind are (Mathews & Baker 1971)

$$\frac{\partial\rho}{\partial t}+\frac{1}{r^2}\frac{\partial}{\partial r}(r^2\rho v)=\alpha\rho_*, \tag{1}$$

$$\rho\left(\frac{\partial v}{\partial t}+v\frac{\partial v}{\partial r}\right)=-\frac{\partial p}{\partial r}-\rho g_*-\alpha\rho_* v, \tag{2}$$

$$\rho\left(\frac{\partial E}{\partial t}+v\frac{\partial E}{\partial r}\right)=-p\frac{1}{r^2}\frac{\partial}{\partial r}(r^2v)-\Lambda(\rho,T)+\alpha\rho_*\left(E_T-E+\frac{v^2}{2}\right), \tag{3}$$

where ρ, v, p, E and T are the density, velocity, pressure, internal energy per unit mass and temperature of the gas respectively.

The total specific mass loss rate is

$$\alpha=\alpha_*+\alpha_{SN}\,.$$

Λ is the volumetric cooling function given below and E_T is the energy injected per unit mass due to both supernovae and random stellar motions

$$E_T=\left(\alpha_{SN}E_{SN}+\alpha\frac{1}{2}\sigma_*^2\right)\Big/\alpha\,. \tag{4}$$

2.2 INITIAL CONDITIONS

We are primarily interested in finding the conditions under which inflow definitely occurs. We therefore choose initial conditions that favour the development of total outflow. We take the initial gas density and temperature to be everywhere $2 \times 10^{-31}\,\mathrm{g\,cm^{-3}}$ and $10^4\,\mathrm{K}$ respectively. These low values mean that there is very little gas in the galaxy to retard the development of outflow and also that the external pressure has no significant effect on any outflow. Finally we take the gas to be initially at rest. These initial conditions may be appropriate if a burst of nuclear activity has cleared the galaxy of stellar mass loss.

2.3 THE COOLING FUNCTION AND EQUATION OF STATE

We assume that the gas lost from stars is optically thin to all radiation. The ionization state of the gas is then determined by collisions alone. Preliminary calculations in which ionization equilibrium was assumed indicated that, when cooling inflow occurs, the temperature changes too rapidly for ionization equilibrium to be maintained if $T < 10^6\,\mathrm{K}$. The general effect of non-equilibrium ionization on the cooling rate is to reduce it below the steady state value (Kafatos 1973; Shapiro & Moore 1976). We adopt a volumetric cooling rate of form

$$\Lambda = n_e\, n_H\, \mathscr{L}(T), \tag{5}$$

where n_e and n_H are the free electron and total hydrogen (i.e. ionized and neutral) number densities respectively. For $10^6 < T \leqslant 10^8\,\mathrm{K}$, $\mathscr{L}(T)$ is determined from the steady state cooling curve of Raymond, Cox & Smith (1976) but with the Fe abundance reduced to that of Cameron (1973). For $10^4 < T < 10^6\,\mathrm{K}$ we use the time-dependent isochoric cooling curve of Shapiro & Moore (1976). Below $10^4\,\mathrm{K}$ we extrapolate the Shapiro & Moore curve in such a way that $\mathscr{L}(T) \to 0$ as $T \to 10^2\,\mathrm{K}$. Below $10^2\,\mathrm{K}$ we take $\mathscr{L} = 0$ and above $10^8\,\mathrm{K}$ we consider only bremsstrahlung cooling. The complete cooling function is shown in Fig. 1 as the curve labelled 'gas'.

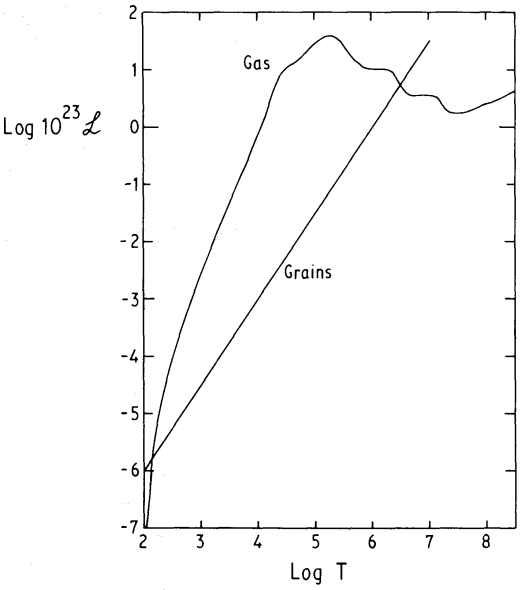

Figure 1. The curve labelled 'gas' is the cooling curve adopted in the numerical calculations. The volumetric cooling rate is $\Lambda = n_e\, n_H\, \mathscr{L}(T)\,\mathrm{erg\,cm^{-3}\,s^{-1}}$ where T is gas temperature in Kelvin. Also shown is the cooling curve for graphite grains.

The calculations of Shapiro & Moore show that hydrogen remains nearly completely ionized down to 10^4 K. Since hydrogen is the main source of electrons we adopt a fully-ionized perfect gas equation of state with mean molecular weight $\mu = 0.585$ appropriate to Cameron (1973) abundances.

2.4 THE GALAXY STRUCTURE

Following Mathews & Baker (1971) we base our galaxy models on the well-studied E1 galaxy NGC 3379. Two galaxy models are considered: a King (1966) model and a de Vaucouleurs (1959) model. In a previous paper (Bailey & MacDonald 1981a) we have used the photometric observations of de Vaucouleurs & Capaccioli (1979) and the spectroscopic observations of Sargent *et al.* (1978) to derive values of the free parameters of these models. The parameters adopted in this work are based on these and are given, together with some derived quantities, in Table 1. For each type of model we calculate self-consistently the stellar density, ρ_*, the gravity, g_*, and the velocity dispersion, σ_*. To avoid numerical difficulties caused by the density singularity at the origin of the de Vaucouleurs law model, we modify the density profile near the centre. We take

$$\rho_* = \rho_a - \rho_b (r/r_e)^2$$

for $r < r_f$. ρ_a and ρ_b are chosen to make density and mass continuous with the de Vaucouleurs law model at the fitting radius r_f, which is taken to be $10^{-3.65} r_e$. This modification affects only the innermost $10^{-6} M_T$.

2.5 METHOD OF SOLUTION

Equations (1), (2) and (3) are solved by the Henyey method (Henyey *et al.* 1959) normally used in stellar evolution studies. The flow is divided into N concentric spherical shells. Scalar quantities, e.g. ρ_*, ρ, T, are evaluated at the midpoints of the shells whereas 'vector' quantities, e.g. r, v, g_*, are evaluated at the shell boundaries. We denote evaluation at the edges of the nth shell by subscripts $n-\frac{1}{2}$ and $n+\frac{1}{2}$ and at the midpoint by subscript n, with $n = 1$ referring to the central spherical zone and $n = N$ referring to the outermost shell. Time derivatives are calculated implicitly, i.e. the derivative of a quantity X at time t is replaced by the finite difference

$$\frac{\Delta X}{\Delta t} \equiv \frac{X(t) - X(t - \Delta t)}{\Delta t}, \tag{6}$$

Table 1. Parameters for the de Vaucouleurs and King models of NGC 3379 as functions of epoch.

Sequence code	A	B	C
Epoch (10^9 yr)	10.0	3.0	1.0
Mass, M_T ($10^{11} M_\odot$)	1.00	1.04	1.09
Luminosity, L_T ($10^{10} L_\odot$)	1.33	2.81	5.86
Specific stellar mass loss rate, α_* (10^{-19} s^{-1})	1.00	3.99	13.3
Total mass loss rate, $\alpha_* M_T$ ($1 M_\odot$ yr^{-1})	0.32	1.31	4.58
Potential energy, $-V$ (10^{59} erg) de Vaucouleurs	1.33	1.49	1.72
King	1.35	1.51	1.74
Effective radius, r_e (1 kpc)	2.17	2.09	1.99
Core radius, r_c (100 pc)	1.32	1.27	1.21
Tidal radius, r_t (1 kpc)	24.7	23.7	22.6
Specific supernova mass loss rate, α_{SN} (10^{-22} s^{-1})	2.00	2.00	2.00
Specific energy of supernova ejecta, E_{SN} (10^{18} erg g^{-1})	2.00	2.00	2.00

where Δt is the time-step. Advective terms, i.e. terms of the form $v\,\partial X/\partial r$, are replaced by upstream differences to ensure numerical stability. Shocks are treated by adding to the gas pressure a pseudo-viscous pressure

$$Q_n = \eta\rho_n\,[3\,(r^2_{n+1/2}\,v_{n+1/2} - r^2_{n-1/2}\,v_{n-1/2})\,(r_{n+1/2} - r_{n-1/2})/(r^3_{n+1/2} - r^3_{n-1/2})]^2,$$

where η is a dimensionless constant which determines the shock thickness. We take $\eta = 2.8$ which spreads shocks over about three meshpoints. The full difference scheme is

$$\frac{\Delta\rho_n}{\Delta t} + \frac{3\,(r^2_{n+1/2}\,v_{n+1/2} - r^2_{n-1/2}\,v_{n-1/2})}{(r^3_{n+1/2} - r^3_{n-1/2})}\,\rho_n + \frac{3\,r^2_{n-1/2}}{r^3_{n+1/2} - r^3_{n-1/2}}\,[v_{n-1/2}]\,(\rho_n - \rho_{n-1})$$

$$- \frac{3\,r^2_{n+1/2}}{r^3_{n+1/2} - r^3_{n-1/2}}\,[-v_{n+1/2}]\,(\rho_{n+1} - \rho_n) = \alpha\rho_{*,n}\,, \tag{7}$$

$$(\rho_n\,\rho_{n+1})^{1/2}\left\{\frac{\Delta v_{n+1/2}}{\Delta t} + [v_{n+1/2}]\,\frac{(v_{n+1/2} - v_{n-1/2})}{(r_{n+1/2} - r_{n-1/2})} - [-v_{n+1/2}]\,\frac{(v_{n+3/2} - v_{n+1/2})}{(r_{n+3/2} - r_{n+1/2})} + g_{*,n+1/2}\right\}$$

$$+ \frac{(P_{n+1} + Q_{n+1} - P_n - Q_n)}{(r_{n+1} - r_n)} + \alpha\rho_{*,n+1/2}\,v_{n+1/2} = 0\,, \tag{8}$$

$$\rho_n\left\{\frac{\Delta\mathscr{E}_n}{\Delta t} + [v_{n-1/2}]\,\frac{(\mathscr{E}_n - \mathscr{E}_{n-1})}{(r_n - r_{n-1})} - [-v_{n+1/2}]\,\frac{(\mathscr{E}_{n+1} - \mathscr{E}_n)}{(r_{n+1} - r_n)}\right\} + \Lambda(\rho_n, T_n)/E_n$$

$$+ \frac{3\,(r^2_{n+1/2}\,v_{n+1/2} - r^2_{n-1/2}\,v_{n-1/2})}{(r^3_{n+1/2} - r^3_{n-1/2})}\,\frac{(P_n + Q_n)}{E_n} - \frac{\alpha\rho_{*,n}}{E_n}\left(E_{T,n} - E_n + \frac{1}{2}v_n^2\right) = 0, \tag{9}$$

where

$$r_n = \frac{1}{2}\,(r_{n+1/2} + r_{n-1/2}),\; v_n = \frac{1}{2}\,(v_{n+1/2} + v_{n-1/2}),\; \mathscr{E}_n = \ln E_n$$

and $[X] = \max(X, 0.0)$ for any X. Note that, although the form of equation (7) conserves mass exactly, momentum and energy are not conserved exactly. Truncation errors are kept small by using a large number, typically 270, of shells. Equations (7), (8) and (9), together with the equation of state, applied to meshpoints 1 to N give $3N$ equations involving $3\,(N + 2)$ unknowns. To complete the set of difference equations boundary conditions and initial conditions are required. At the centre of the flow ($r_{1/2} = 0$) we have $v_{1/2} = 0$. Hence ρ_0 and E_0 which appear in equations (7) and (9) applied at $n = 1$ can be given any finite value. We set $\rho_0 = \rho_1$ and $E_0 = E_1$. At time $t = 0$, we are free to specify the run of ρ, T and v in the flow. Since we are interested in the development of the flow due to mass loss from stars we assume any gas initially in the galaxy is at rest and has low density and pressure. We take the initial density and temperature to have the values given in Section 2.2. The outer edge of the flow is taken to be at large but fixed radius (typically 10^3 effective radii). Material outside the outer edge is assumed to remain at rest and have density and temperature equal to the initial values. This fixes ρ_{N+1}, T_{N+1}, $v_{N+3/2}$. The complete set of non-linear difference equations is solved iteratively using a program kindly lent by Dr Peter Eggleton.

3 Evolution of elliptical galaxies: a simple model

3.1 THE STELLAR MASS LOSS RATE

To study how the strength of nuclear activity may depend on epoch we need to know how the galaxy and, in particular, α_* and α_{SN} evolve with time. We assume that star formation occurs instantaneously and simultaneously throughout the galaxy at time $t = 0$ and that no further star formation occurs. We further assume that there is no residual gas from star formation and that gas lost from stars is ultimately ejected from the galaxy either by a galactic wind or, in the case of inflow, by the nuclear activity itself.

The initial stellar mass function is taken to be of form

$$\phi(m) = km^{-(1+\beta)},\ m_L \leqslant m \leqslant m_U \tag{10}$$

and zero otherwise. $\phi(m)dm$ is the number of stars which have masses in the interval $(m, m + dm)$. k is related to $M_T(0)$, the initial total galaxy mass by ($\beta \neq 1$)

$$M_T(0) = \frac{k}{\beta - 1}\left(\frac{1}{m_L^{\beta-1}} - \frac{1}{m_U^{\beta-1}}\right). \tag{11}$$

Stellar mass loss is assumed to occur instantaneously at the end of a star's main-sequence lifetime $\tau(m)$. Thus, if a star of initial mass m loses a mass $\lambda(m)$ during its lifetime the total mass loss rate is

$$\frac{dM_T}{dt} = \phi(m')\,\lambda(m')\left(\frac{d\tau}{dm}\bigg|_{m=m'}\right)^{-1}, \tag{12}$$

where $t = \tau(m')$.

We adopt an approximation given by Tinsley (1976) for $\lambda(m)$, and use Larson's (1974a) expression for $\tau(m)$ in years.

$$\begin{aligned} \lambda(m) &= 0.84m - 0.44 \qquad 1 \leqslant m \leqslant 6 \\ &= \quad m - 1.4 \qquad\ \ 6 \leqslant m \end{aligned} \tag{13}$$

$$\log\tau(m) = 10.02 - 3.57\log m + 0.90(\log m)^2. \tag{14}$$

In the above, m and λ are measured in solar masses. Equation (12) is easily integrated to give $M_T(m')$.

Further progress requires knowledge of the parameters describing the initial mass function. We take $\beta = 1.35$ (Salpeter 1955) and $m_U = 50$. The lower limit, m_L, is chosen so that the present-day ($t = 10^{10}$ yr) M/L ratio for the galaxy agrees with the observations of NGC 3379. Using the mass–luminosity relation for stars, $L/L_\odot = m^{3.45}$ (Allen 1973) and $M_T/L_T = 7.5$ in solar units (Bailey & MacDonald 1981a) we find $m_L = 0.127$. The initial mass of our model galaxy is then found to be $M_T(0) = 1.42 \times 10^{11} M_\odot$.

The present day mass loss rate is $0.32 M_\odot \mathrm{yr}^{-1}$ in good agreement with the mass loss rate adopted as standard by Faber & Gallagher (1976). In Fig. 2 we give graphs of the specific stellar mass loss rate, $\alpha_* = -(1/M_T)\,dM_T/dt$, and the fractional galaxy mass, $f = M_T/M_T(0)$, as functions of time. We note that if stellar mass loss is able to flow inwards and fuel nuclear activity, the amount of fuel made available in the interval $10^8 \leqslant t \leqslant 10^{10}$ yr is $\simeq 0.14 M_T(0) = 2.0 \times 10^{10} M_\odot$. If this amount of fuel is converted into energy at only nuclear-reaction efficiencies (0.7 per cent) the energy released is in excess of 2×10^{62} erg. This suggests that stellar mass loss is a sufficient source of fuel to power even the most energetic radio sources (De Young 1976).

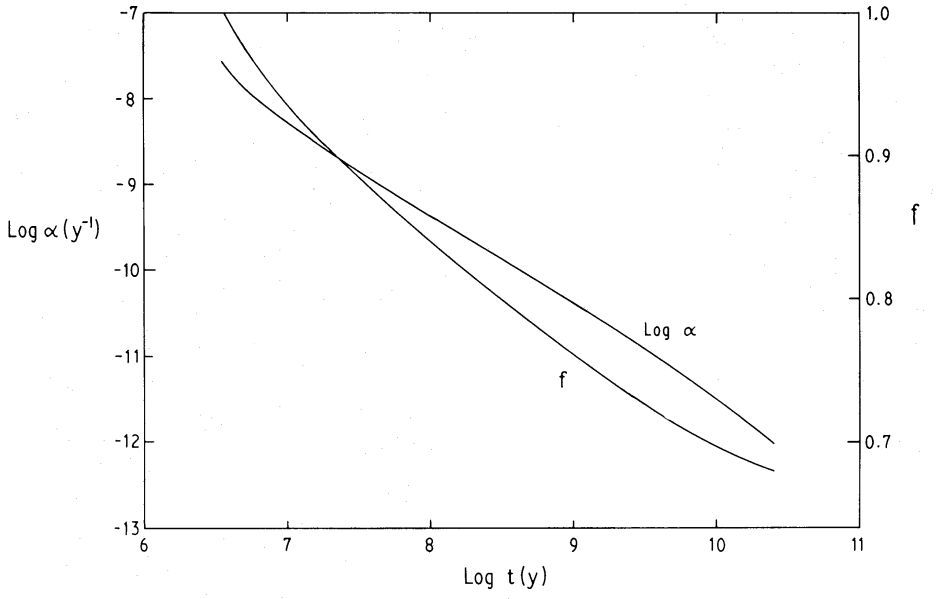

Figure 2. Specific stellar mass loss rate, α, and fractional galaxy mass, f, as function of epoch, t.

A further consequence of mass loss from the galaxy is that it becomes less tightly bound and hence increases in radius. We assume that the galaxy evolves quasi-statically and homologously. Radii then scale as M_T^{-1} and velocity dispersions as M_T. The values of M_T, α_*, effective radius of the de Vaucouleurs model, r_e, core radius of the King model, r_c, for our particular galaxy models are shown for three different epochs in Table 1.

3.2 SUPERNOVA HEATING AND OTHER ENERGY SOURCES

To complete the model we need to know the specific mass loss rate for supernovae, α_{SN}, and the energy per unit mass injected into the flow by supernovae, E_{SN}. At present it is not possible to make a completely justifiable assumption about the evolution of the supernova rate in elliptical galaxies because of uncertainty in the mass range of type I supernova progenitors (Tammann 1974, 1977; Tinsley 1977; Oemler & Tinsley 1979). Oemler & Tinsley (1979) have suggested that type I supernovae have massive, short-lived progenitors. If this is the case, a supernova-driven wind would be self-defeating; it would remove the material necessary for making new supernovae to drive the wind. Instead periods of outflow, separated by periods in which the stellar mass loss can cool and flow inwards, may occur. We do not consider this possibility here but make the more conventional assumption that type I supernovae have long-lived, low-mass progenitors (Shklovskii 1978). We adopt the observed value (Tammann 1977)

$$\nu_{SN} = 0.19\,(H_0/55\,\mathrm{km\,s^{-1}\,Mpc^{-1}})^2\,(L_T/10^{10}L_\odot)(100\,\mathrm{yr})^{-1}$$

for the supernova rate in elliptical galaxies of luminosity L_T. The total kinetic energy of the ejecta of a type I supernova is typically 4×10^{50} erg (Gorenstein & Tucker 1976). Adopting an ejection velocity of $2\times10^4\,\mathrm{km\,s^{-1}}$ (Searle 1974), corresponding to $E_{SN} = 2\times10^{18}\,\mathrm{erg\,g^{-1}}$, gives the total mass ejected per supernova, $M_{ej} = 0.1\,M_\odot$. Taking $L_T = 1.33\times10^{10}L_\odot$ and $H_0 = 85\,\mathrm{km\,s^{-1}\,Mpc^{-1}}$ (de Vaucouleurs & Capaccioli 1979) we find $\alpha_{SN} = 2\times10^{-22}\,\mathrm{s^{-1}}$.

In view of the above-mentioned uncertainties, we make the simplest assumption that α_{SN} and E_{SN} are independent of epoch. In fact, if type I supernovae are due to dynamical collapse of white dwarfs (Wheeler & Hansen 1971) accreting material from a low-mass binary

companion (Whelan & Iben 1973), α_{SN} may increase with time because of the long evolutionary time-scale of the companion. In the next section we show that it is essentially the ratio α_{SN}/α that determines whether or not inflow occurs. Hence, provided α_{SN} does not decrease as rapidly as α, inflow will occur at some epoch earlier than the present.

Coleman & Worden (1976) have suggested that flare stars are a major source of energy and mass in elliptical galaxies. However, their result depends crucially on the fraction of dwarf M stars that are active flare stars. Using the data of Joy & Abt (1974) for solar neighbourhood stars, Coleman & Worden (1976) concluded that about 50 per cent of stars later than dM2 are active. Kunkel (1975) gives strong evidence that the duration of the flare active stage of a low mass star is a monotonically increasing function of absolute magnitude and is comparable to the age of the Galaxy for stars fainter than $M_v = 15$. Hence in an elliptical galaxy, in which no star formation has been going on, only the very low luminosity stars of spectral type later than M7 will be flare active after 10^{10} yr. Since f_{flare}, the fraction of stellar energy expended in flare activity is between 0.1 and 1 per cent, irrespective of spectral type (Kunkel 1973), Coleman & Worden (1976) may have substantially overestimated the importance of flare stars as an energy source in elliptical galaxies at late epochs. The situation is complicated by the fact that stars in binaries have a prolonged active stage (Kunkel 1975). However, even if we assume 50 per cent of M stars are in binaries and hence are active, and that $f_{flare} = 0.003$ we find a flare star energy input rate of $3.8 \times 10^6 L_\odot$ for a $10^{11} M_\odot$ galaxy, a factor 5 less than our supernova heating rate. Hence we do not include in our models an energy source term due to flare stars. Flare-star-driven winds have been considered in detail by Coleman & Worden (1977).

4 Approximate analytic results

To get some insight into the conditions under which a total or partial wind is possible, it is worth considering the global energy balance of a steady flow. Suppose there is a 'stagnation point', at which $v = 0$, in the flow at radius r_s. From equations (1), (2) and (3) the steady state energy flux equation can be derived

$$\frac{1}{r^2}\frac{d}{dr}\left\{r^2\rho v\left(E+\frac{p}{\rho}+\frac{1}{2}v^2\right)\right\} = -\Lambda - v\rho g_* + \alpha\rho_* E_T . \tag{15}$$

Using the fact that the galaxy is in hydrostatic equilibrium, multiplying equation (15) by $4\pi r^2$ and integrating from r_s to infinity gives a global energy equation for the flow outside r_s

$$\alpha\,[M_T - m_*(r_s)]\left(E+\frac{p}{\rho}+\frac{1}{2}v^2\right)\Big|_\infty = -L_{gas}(r_s) + \alpha_{SN} E_{SN}\,[M_T - m_*(r_s)]$$
$$-\frac{3}{2}\alpha\int_{m_*(r_s)}^{M_T}\frac{Gm_*\,dm_*}{r} - \frac{2\pi}{3}\alpha r_s^3(\rho_*\sigma_*^2)\Big|_{r_s} - \alpha\left[\frac{Gm_*^2(r_s)}{r_s} - m_*(r_s)\int_{r_s}^{\infty}\frac{Gm_*\,dr}{r^2}\right], \tag{16}$$

where $L_{gas}(r)$ is the luminosity of the gas outside radius r and $m_*(r)$ is the mass of stars within r. Since $L_{gas} > 0$, we see that a necessary condition for the existence of a steady state solution with stagnation radius r_s is

$$\alpha_{SN} E_{SN}\,[M_T - m_*(r_s)]/\alpha > \frac{3}{2}\int_{m_*(r_s)}^{M_T}\frac{Gm_*\,dm_*}{r} + \frac{2\pi}{3}r_s^3(\rho_*\sigma_*^2)\Big|_{r_s}$$
$$+\frac{Gm_*^2(r_s)}{r_s} - m_*(r_s)\int_{r_s}^{\infty}\frac{Gm_*\,dr}{r^2} . \tag{17}$$

A case of particular interest is that of a total wind for which $r_s = 0$. The condition (17) then becomes

$$\alpha_{SN} E_{SN} M_T/\alpha > \frac{3}{2}\int_0^{M_T} \frac{Gm_* dm_*}{r} \equiv \frac{3}{2}|V|, \tag{18}$$

where V is the potential energy of the galaxy.

Let

$$\gamma = \frac{2}{3}\alpha_{SN} E_{SN} M_T/\alpha|V|,$$

condition (17) can then be written

$$\gamma > F(s), \tag{19}$$

where F is a dimensionless function of dimensionless radius, s (e.g. $s = r/r_e$ for a de Vaucouleurs galaxy, $s = r/r_c$ for a King model). The function F is shown plotted against r/r_e in Fig. 3 for both types of model. For the King model we have taken $r_t/r_c = 187$, the value used in the wind calculations.

Since the galaxy is in hydrostatic equilibrium the potential energy is related to the mean line-of-sight velocity dispersion of the galaxy, $\bar{\sigma}$, by

$$|V| = 3M_T \bar{\sigma}^2. \tag{20}$$

Hence galaxies with $\bar{\sigma}^2 > 2\alpha_{SN}E_{SN}/9\alpha$ will have inflow of stellar mass loss. Using our values of α_{SN}, E_{SN}, and the present epoch value of α, we find that inflow will be going on in nearby galaxies with mean line-of-sight velocity dispersion greater than 300 km s^{-1}. Also the greater the value of $\bar{\sigma}$, the greater will be r_s, and hence inflow rate. Hence we might expect galaxies with high $\bar{\sigma}$ to be more active than galaxies with low $\bar{\sigma}$. Since, as pointed out by Faber & Gallagher (1976), the optical luminosity of elliptical galaxies is correlated with $\bar{\sigma}$, roughly as $L_T \propto \bar{\sigma}^4$, this gives a natural explanation for the correlation between strength of radio emission and optical luminosity of elliptical galaxies as found by Ekers & Ekers (1973)

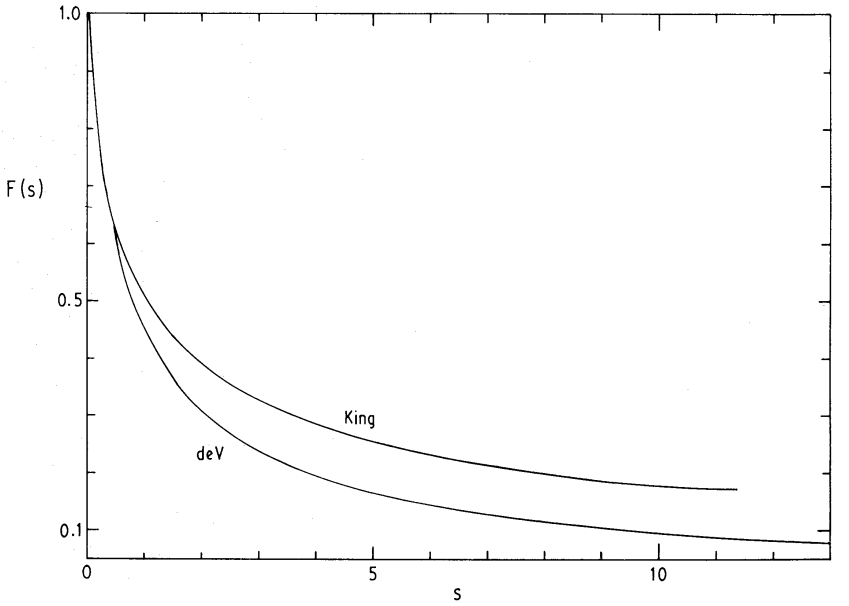

Figure 3. The function F that appears in the partial wind criterion plotted against dimensionless radius $s = r/r_e$ for both the King and de Vaucouleurs galaxy models.

and Colla *et al.* (1975). A detailed discussion of the relevance of the energy balance criterion to radio source number density evolution can be found in Bailey & MacDonald (1981b).

Some idea of when cooling is an important factor in determining whether total outflow ($r_s = 0$) can occur can be obtained by considering the case $\gamma \gg 1$ (formally equivalent to $G \to 0$). First suppose that cooling is negligible. The flow equations can then be reduced to the single wind equation

$$(4u^2 - 1)\frac{du}{dx} = -u(4u^2 + 1)\frac{d\ln m_*}{dx} + 2u(1 - u^2), \tag{21}$$

where

$$u^2 = \frac{\alpha}{\alpha_{SN}}\frac{v^2}{2E_{SN}}$$

and

$$x = \ln r.$$

The sonic point, $u = {}^1/_2$, occurs where

$$\frac{d\ln m_*}{dx} = {}^3/_4.$$

The central gas temperature is

$$T_c = \frac{2}{5}\frac{\mu}{\mathscr{R}}\frac{\alpha_{SN}E_{SN}}{\alpha}. \tag{22}$$

For typical values of $\alpha_{SN}E_{SN}/\alpha$ we find $T_c \sim 10^{6.5}$ K. The cooling rate for $10^{5.3} \lesssim T \lesssim 10^{7.5}$ K can be approximated by

$$\Lambda = 1.33 \times 10^{29}\rho^2 T^{-0.6}\,\mathrm{erg\,cm^{-3}\,s^{-1}}. \tag{23}$$

Solving equation (21) numerically and integrating the approximation (23) over the flow gives the total gas luminosity for the King model

$$L_{gas}^{K} = 1.20 \times 10^{27}\frac{\alpha^3}{\alpha_{SN}E_{SN}}\frac{M_T^2}{r_c}\frac{1}{T_c^{0.6}}\,\mathrm{erg\,s^{-1}}. \tag{24}$$

Comparing this with the total supernova heating we see that cooling is important if

$$\alpha_{SN}E_{SN} < 2.44 \times 10^{12}\alpha^{18/13}\left(\frac{M_T}{r_c}\right)^{5/13}\mathrm{erg\,g^{-1}\,s^{-1}}. \tag{25}$$

Similarly for the de Vaucouleurs law galaxy we find the condition

$$\alpha_{SN}E_{SN} < 6.78 \times 10^{12}\alpha^{18/13}(M_T/r_e)^{5/13}\,\mathrm{erg\,g^{-1}\,s^{-1}}. \tag{26}$$

Since $r_e = 16.4\,r_c$ for our models of NGC 3379, conditions (25) and (26) are essentially equivalent.

In Fig. 4 we plot the conditions (18) and (26) in the ($\log M_T/r_e$–$\log\alpha$) plane, together with the evolutionary track of NGC 3379. The mean line-of-sight velocity dispersion for the whole galaxy

$$\bar{\sigma} = 0.335\,(GM_T/r_e)^{1/2}$$

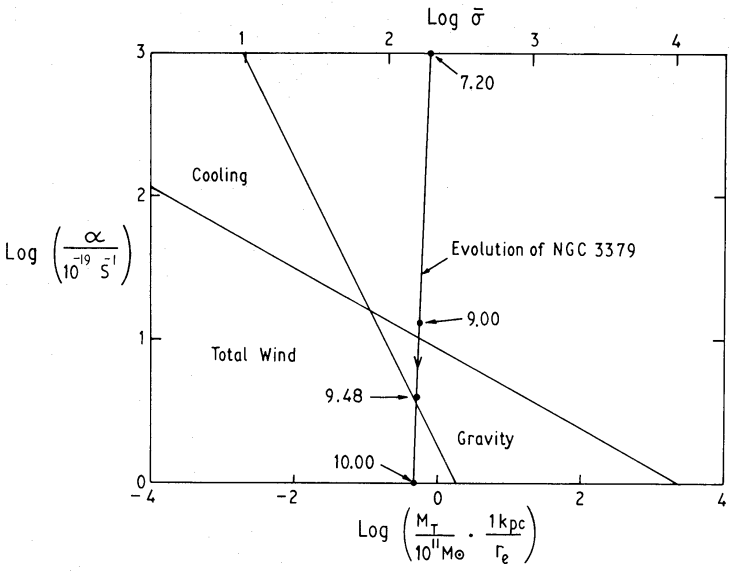

Figure 4. The evolutionary track of our model for NGC 3379 in the ($\log\alpha$–$\log M_T/r_e$) plane. The filled circles are labelled by log t, where t is epoch in yr. Also shown are the regions in which radiative cooling and gravity prevent total outflow, and in which total outflow can occur, according to the analytic results of Section 4. $\alpha_{SN} E_{SN} = 4 \times 10^{-4}$ erg g^{-1} s^{-1} has been assumed.

is also shown. $\alpha_{SN} E_{SN} = 4 \times 10^{-4}$ erg g^{-1} s^{-1} has been assumed. We see from Fig. 4, that for galaxies with $\bar{\sigma} \lesssim 75$ km s^{-1}, cooling is the major factor in determining whether inflow or total outflow occurs. For more tightly bound galaxies it is the balance between gravity and supernova heating that decides the issue.

5 Results of the numerical calculations

We have followed numerically the development of the gas flow in both the King and de Vaucouleurs models of NGC 3379 at the three epochs given in Table 1. We discuss first the present epoch ($t = 1 \times 10^{10}$ yr) models (hereafter referred to as sequence DA for the de Vaucouleurs galaxy model and sequence KA for the King galaxy model), and then the models for the earlier epochs (sequences DB, KB at $t = 3 \times 10^9$ yr and sequences DC, KC at $t = 1 \times 10^9$ yr).

5.1 PRESENT EPOCH MODELS

As predicted by condition (18), steady state outflow develops in both sequence DA and sequence KA. The evolution towards the steady states is shown in Figs 5(a)–(c) (sequence KA) and 6(a)–(c) (sequence DA) in which gas density in units of 10^{-30} g cm^{-3}, gas temperature in Kelvin and gas velocity in units of 100 km s^{-1}, respectively are plotted against radius in parsecs at different times after the start of the calculation. Some physically interesting parameters of the steady outflows are given in Table 2.

Sequence KA is qualitatively similar to the steady outflow model of Mathews & Baker (1971); the differences in the velocity profile at early times are due to the different choice of initial conditions. The major difference between sequences DA and KA is the much larger velocities of sequence DA at radii less than 100 pc. This is due to the much higher central star density of the de Vaucouleurs galaxy model which results in a much larger mass input rate within the inner 100 pc of the galaxy, and also a smaller dynamical time-scale.

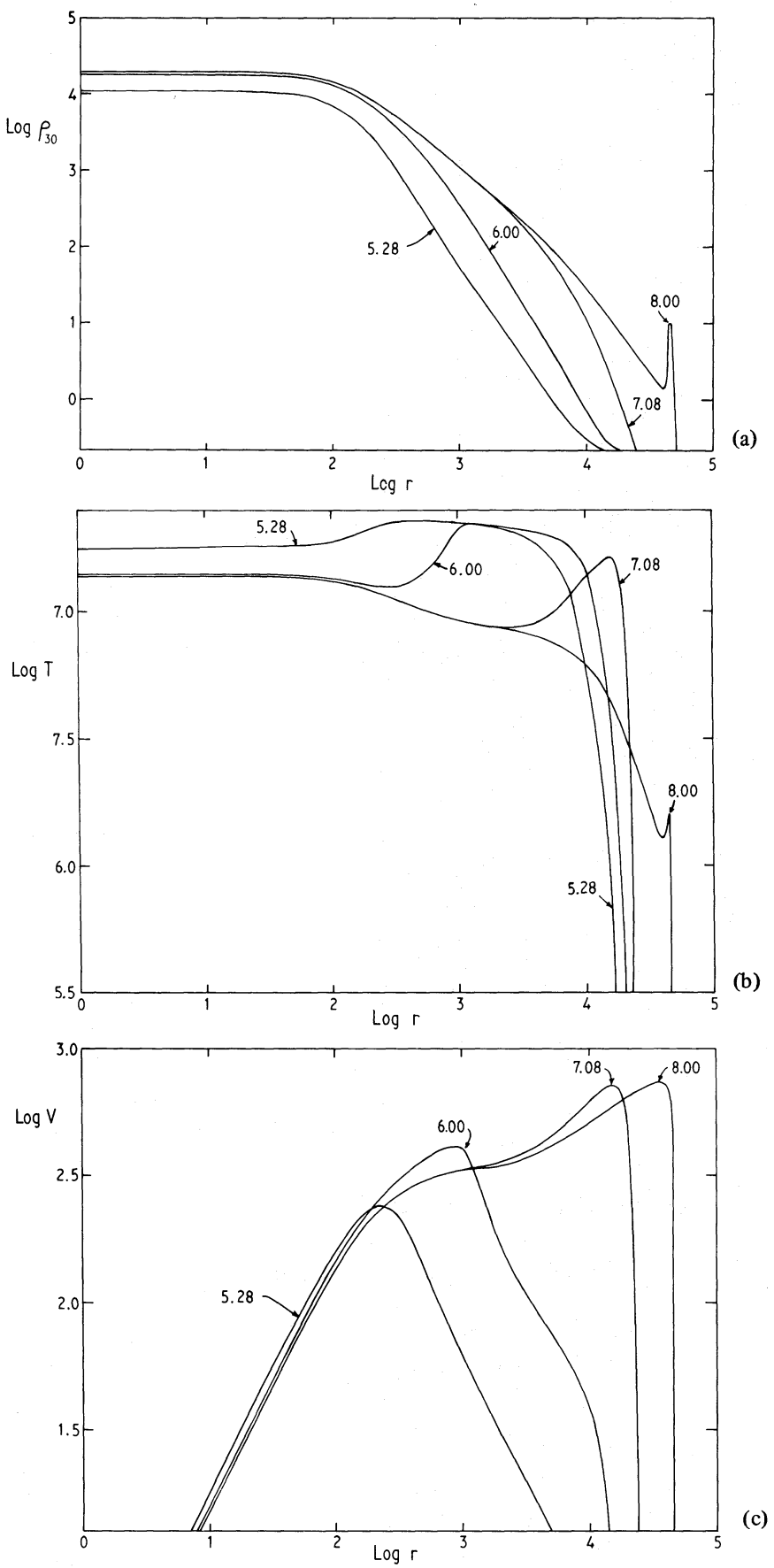

Figure 5. Plots of (a) gas density, (b) temperature and (c) velocity against radius for sequence KA at various times, ρ_{30} is the gas density in units of 10^{-30} g cm^{-3}, T is gas temperature in Kelvin, V is gas velocity in km s^{-1} and r is radius in pc. The curves are labelled with log t, where t is the time in yr.

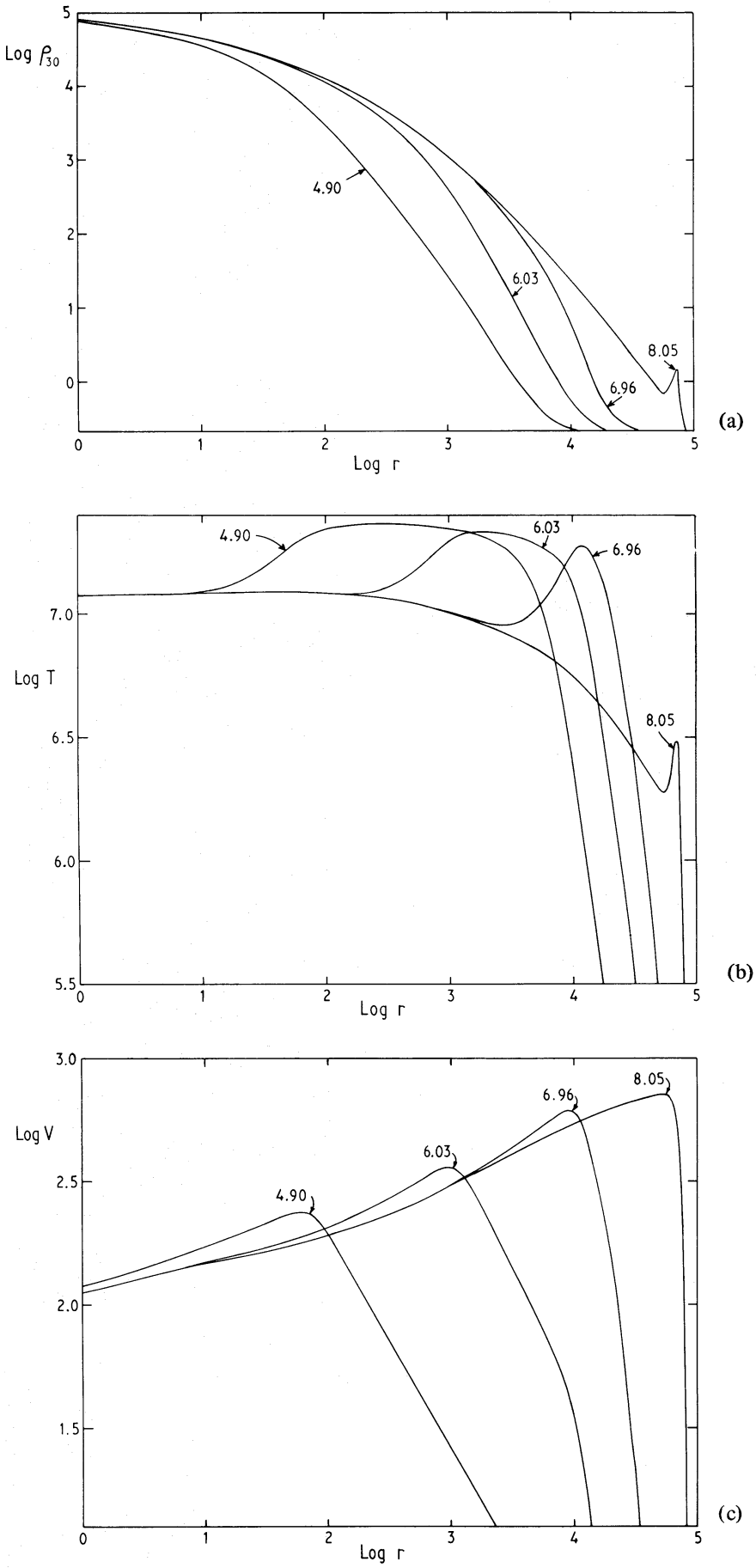

Figure 6. (a)–(c) As Fig. 5(a)–(c) but for sequence DA.

Table 2. Parameters of total outflows.

Sequence	KA	DA
T_c (10^7 K)	1.378	1.190
T_{in} (10^7 K, centre)	2.301	1.988
ρ_c (10^{-26} g cm^{-3})	1.980	10.73
t_f (10^4 yr, centre)	30	0.2
$\alpha\rho_* t_f$ (10^{-26} g cm^{-3})	3	18
L_{gas} ($10^3 L_\odot$)	3.98	3.63
M_{gas} (2 kpc) ($10^5 M_\odot$)	3.80	3.93
M_{gas} (20 kpc) ($10^6 M_\odot$)	9.11	8.05

The characteristic time for development of outflow at radius r is a dynamical time-scale

$$t_f \simeq \left\{\left(\frac{\bar{T}_{in}}{\bar{T}_*} - 1\right) G\bar{\rho}_*\right\}^{-1/2}. \tag{27}$$

Here $\bar{T}_{in}$ is the mean temperature of the injected gas, $\bar{\rho}_*$ is the mean density of stars within r and $\bar{T}_*$ is the gas temperature corresponding to the mean velocity dispersion of stars within r. The time to reach equilibrium will also be $\sim t_f$ and hence ρ_c, the central gas density, will be $\sim \alpha\rho_* t_f$ evaluated at the centre. The values found in the numerical calculations are in good agreement with this rough estimate.

In the absence of cooling an exact expression for the central gas temperature is

$$T_c = \frac{3}{5} T_{in} \equiv \frac{2}{5}\frac{\mu E_t}{\mathscr{R}}. \tag{28}$$

The computed values are slightly less than this because of the small amount of cooling.

Equation (24), and its counterpart for the de Vaucouleurs law galaxy, give a rough estimate for the total luminosity of the gas, $L_{gas} \simeq 4 \times 10^3 L_\odot$ which agrees surprisingly well with the values found in the last computed model for the luminosity of the outflowing gas. Also given in Table 2 are the masses of gas contained with 2 and 20 kpc.

The observability of a hot total outflow has been discussed by Mathews & Baker (1971) who concluded that such a wind should be totally undetectable except possibly for infrared emission from dust grains ejected from stars. Comparison of flow times with sputtering time-scales for graphite grains (Burke & Silk 1974) indicates that destruction of grains by sputtering in the hot outflowing gas is negligible. Hence, if a fraction, f_g, of the carbon ejected by stars is in the form of grains, the cooling per unit volume due to grain–gas collisions, Λ_{grains}, is (for $T \lesssim 10^7$ K)

$$\Lambda_{grains} \simeq 7 \times 10^{-24} f_g \left(\frac{\rho}{M_H}\right)^2 \left(\frac{T}{10^6\,\mathrm{K}}\right)^{3/2} \left(\frac{0.1\,\mu\mathrm{m}}{a}\right) \mathrm{erg\,cm^{-3}\,s^{-1}}, \tag{29}$$

where M_H is the mass of a hydrogen atom and a is the radius of a typical grain (Burke & Silk 1974). Taking $f_g = 1$ and $a = 0.1\,\mu$m, this can be written in the same form as the gas cooling law,

$$\Lambda_{grains} = n_e n_H \mathscr{L}_{grains}(T), \tag{30}$$

where

$$\mathscr{L}_{grains}(T) = 10^{-23} \left(\frac{T}{10^6}\right)^{3/2} \mathrm{erg\,cm^3\,s^{-1}}. \tag{31}$$

$\mathscr{L}_{\text{grains}}(T)$ is shown in Fig. 1. Hence, for $T \gtrsim 3 \times 10^6$ K, grain cooling may be greater than gas cooling and we need to check that it is negligible compared to the supernova heating. Integrating the grain cooling over the steady state outflow we find a luminosity $L_{\text{grain}} \simeq f_g\, 4 \times 10^4 L_\odot$ for both sequences DA and KA. This is much less than the supernova heating ($\simeq 2 \times 10^7 L_\odot$) and hence cooling by grain–gas collisions does not upset the steady outflow. The grain temperature, $\simeq 15$ K, is such that the IR dust emission peaks at a wavelength of $\simeq 250\,\mu$m. We estimate that, at this wavelength, the dust emission is only about 10 times that of the stars and hence is probably undetectable.

We conclude that steady outflowing winds are not directly observable. They may, however, be detected indirectly by their interaction with the intergalactic medium (IGM). As the wind evolves, a shock front develops, sweeping up the IGM to form a hot, dense shell (see Figs 5a and 6a). Such shells may have already been detected around giant elliptical galaxies (Malin & Carter 1980).

5.2 EARLY EPOCH MODELS

As predicted by condition (18), steady total outflow develops in none of the early epoch sequences, DB, KB, DC and KC. This is simply because supernovae do not provide enough energy to eject matter from the deep potential well of the central regions of the galaxy. Instead material accumulates in the central regions until the density becomes high enough for the gas to cool rapidly. The decrease in pressure results in inflow of material. In the outer, less tightly bound parts of the galaxy supernovae can still supply enough energy to drive gas out and hence a partial wind develops.

Figs 7 and 8 show the evolution of density, temperature and velocity of the gas for sequences KC and DC respectively. The overall development of sequences KB and DB is similar.

The early evolution of sequences KB and KC is similar to that of sequence KA in that outflow begins at the centre. However, the velocities do not become large enough to set up a steady-state density distribution, and so the density continues to increase. Cooling by adiabatic expansion is unimportant and hence the gas temperature remains near the temperature of the injected gas

$$T_{\text{in}} = \frac{2}{3}\frac{\mu}{\mathscr{R}} E_{\text{T}} . \tag{32}$$

For sequences KB and KC, within one core radius of the centre, $T_{\text{in}} \simeq 8 \times 10^6$ K and 5×10^6 K respectively. Cooling becomes important when the density is such that

$$\Lambda(T_{\text{in}}) \sim \alpha_{\text{SN}} E_{\text{SN}} \rho_* \tag{33}$$

which gives $\rho \simeq 10^{-24}\,\text{g cm}^{-3}$ for both sequences.

Since this density is attained first at the centre, inflow begins there at times 8.4×10^6 and 1.1×10^6 yr for sequences KB and KC, respectively. Because the denser gas cools faster a situation develops in which, although density decreases outwards, the pressure increases outwards. It is this pressure gradient that is responsible for most of the acceleration as the gas moves towards the centre. When the gas temperature is $\sim 3 \times 10^5$ K, i.e. near the peak of the cooling curve, the gas cools rapidly to $\sim 10^4$ K. This leads to an outward moving cooling front (see Figs 7b, 8b). Immediately after the rapid cooling, pressure forces are negligible and the gas supersonically free falls for a short period. As the gas continues to fall inwards it is compressed and pressure forces again become non-negligible. A shock develops at the centre and slowly moves outward. For the extent of the calculations this shock remains within 1.3 pc of the centre for sequence KB and within 1.2 pc for sequence KC.

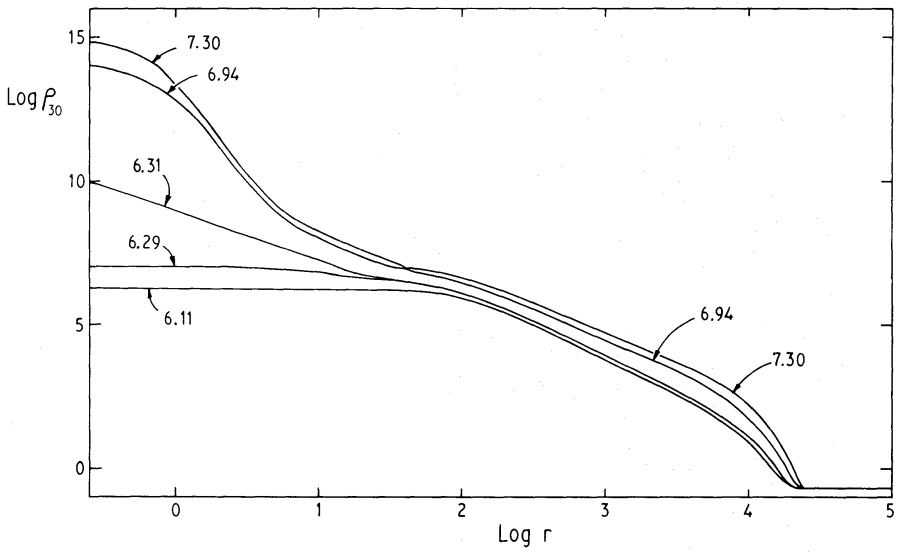

(a)

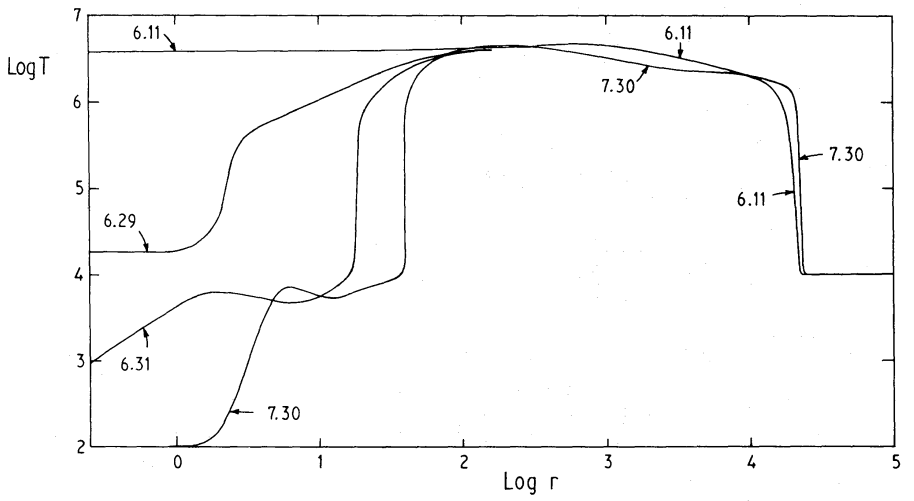

(b)

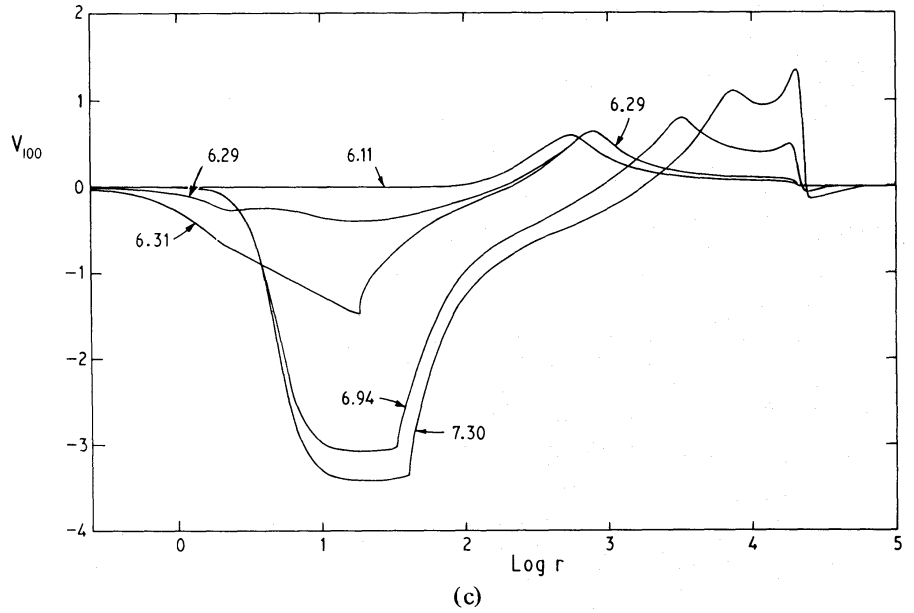

(c)

Figure 7. (a)–(c) As Fig. 5(a)–(c) but for sequence KC, V_{100} is the gas velocity in units of 100 km s^{-1}.

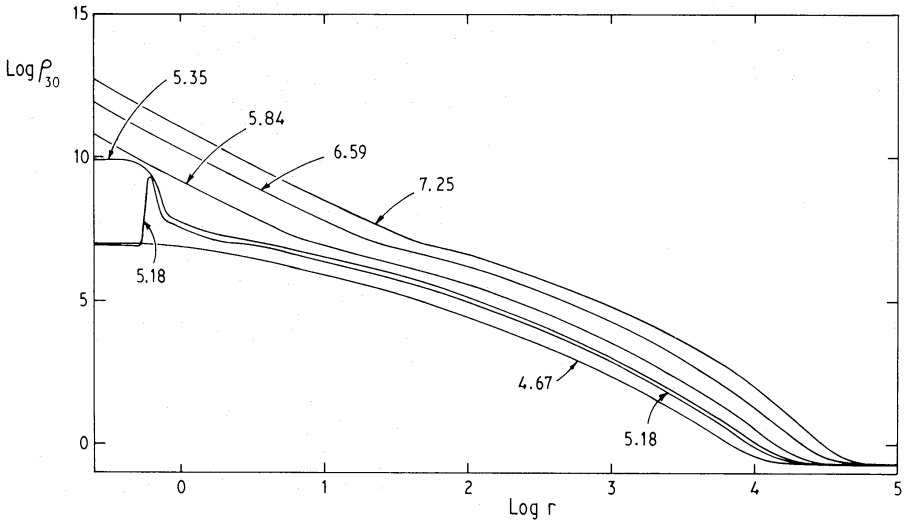

(a)

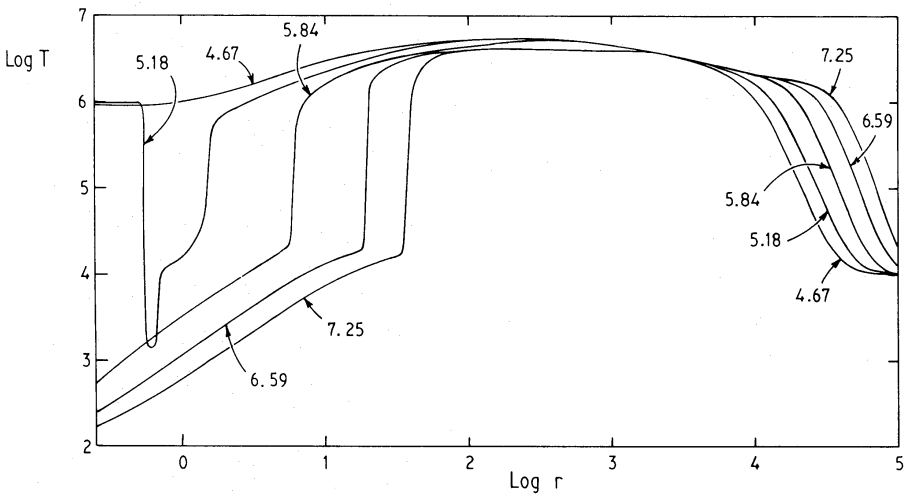

(b)

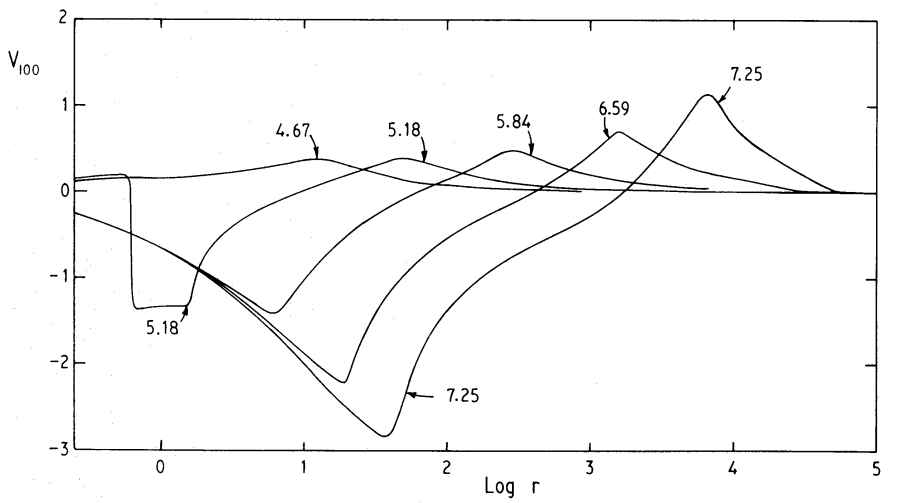

(c)

Figure 8. (a)–(c) As Fig. 7 but for sequence DC.

Another consequence of the pressure increasing outwards is that the gas is prone to Rayleigh–Taylor instability. However, the growth time for perturbations of wavelength equal to the density scale height is at least a factor of 2 greater than the time to completely traverse the unstable region, $\sim 10^5$ yr. Hence it is not unreasonable to neglect the effects of the instability on the flow.

In sequence KB the stagnation radius, r_s, at first moves rapidly outwards reaching 209 pc at 1.08×10^7 yr. As the density in the central regions further increases, r_s continues to move outwards but more slowly, reaching 300 pc at 1.76×10^7 yr. Condition (19) gives a lower limit on r_s of 169 pc. However, this limit is for a steady flow and is obtained by neglecting cooling which is necessary for there to be any inflow at all. Hence the values for r_s found in the numerical calculation are somewhat higher than given by condition (19). It is clear from the numerical calculations that as the density in the central regions continues to increase, r_s will continue to move outwards on a time-scale 10^7 yr, i.e. about one flow time.

In Table 3 we give some parameters of the inflow models at the end of the calculations, taken arbitrarily to be at 1.76×10^7 yr. This is longer than the time at which the nature of the flow will be changed by self-gravitation of the gas becoming important at the centre. $M_{\mathrm{gas,s}}$ is the mass of gas inside the stagnation radius r_s and F_s $(=\alpha m_*(r_s))$ is the total inflow rate. $M_{\mathrm{gas,t}}$ and $L_{\mathrm{gas,t}}$ are the total mass and luminosity of the gas inside the galaxy.

The evolution of sequence KC is similar to that of sequence KB. Because of the higher specific mass loss rate and hence lower specific energy of the injected material, the inflow starts earlier and involves a greater part of the galaxy. Again r_s moves out rapidly at first, reaching 536 pc at 4.23×10^6 yr, but then slows down, reaching 1.59 kpc at the end of the calculations.

The evolution of sequences DB and DC differs from the King models in that inflow begins away from the centre. This is because the very high central star density results in a high supernova heating rate that dominates the gas cooling. The stellar density drops rapidly with increasing r and cooling becomes more effective. Again cooling becomes important when $\Lambda \sim \alpha_{\mathrm{SN}} E_{\mathrm{SN}} \rho_*$. The resultant local drop in pressure causes material to flow into the cooling region from both sides. This results in a sharp increase in density which further increases the cooling. Thus a cool, dense gas shell forms above a hotter, less dense interior which tries to support it against gravity. This is again a situation that may result in Rayleigh–Taylor instability. The growth time for perturbations of wavelength equal to the density scale height, $\sim 10^4$ yr, is now much less than the time for which the shell is Rayleigh–Taylor unstable. Hence the shell may break up into cold blobs that sink towards the centre, with the hot interior gas moving outwards around them. We have not tried to model the behaviour of this two-component medium but instead have continued the evolution, ignoring the Rayleigh–Taylor instability.

In sequence DB the high-density, cold shell forms at $r = 4.2$ pc when $t = 2.78 \times 10^6$ yr. By $t = 4.80 \times 10^6$ yr the shell has fallen to the centre. The subsequent evolution is similar to that of sequence KB, the main difference being that, at comparable times, the stagnation

Table 3. Parameters of partial inflows at $t = 1.76 \times 10^7$ yr.

Sequence	KB	KC	DB	DC
r_s (1 kpc)	0.30	1.6	0.23	1.7
$M_{\mathrm{gas,s}}$ $(10^7 M_\odot)$	0.12	2.4	0.071	2.7
F_s $(1 M_\odot \mathrm{yr}^{-1})$	0.10	1.5	0.064	1.7
$M_{\mathrm{gas,tot}}$ $(10^7 M_\odot)$	2.3	8.1	2.6	8.3
$L_{\mathrm{gas,tot}}$ $(10^7 L_\odot)$	0.38	4.4	0.23	6.7

radius is larger for the King model. This difference can be attributed to the difference in structure of the underlying galaxy and is as expected from the analytic criterion, equation (19), for steady flows.

Sequence DC differs from sequence DB in that inflow begins much earlier and much closer to the Galactic Centre. Again the higher mass loss rate is responsible as it gives a lower mean temperature for the injected material and a faster build-up of the gas density, so that supernova heating is overcome earlier. Inflow begins at $r = 1.37$ pc when $t = 7.22 \times 10^4$ yr. Again a dense cold shell forms and falls inwards, reaching the centre at $t = 2.25 \times 10^5$ yr. The evolution is then qualitatively similar to sequence KC. The difference in positions of the stagnation radius is, however, not as marked as for sequences DB and KB.

By comparing the flows in the de Vaucouleurs and King model galaxies we see that, although there are differences in the details of the flows, the global properties of the flows, e.g. the total inflow rate, do not depend critically on the detailed structure of the underlying galaxy but are essentially determined by the values of the specific mass loss rate, supernova heating and the global properties of the galaxy, e.g. its potential energy.

5.3 VALIDITY OF ASSUMPTIONS AND APPROXIMATIONS

In our model for the gas flow in elliptical galaxies a number of assumptions and approximations, not all of which have been stated explicitly, have been made. In this section we check the validity of these approximations.

Throughout the calculations we have assumed that all the kinetic energy of the supernovae goes into heating the interstellar medium (ISM). As pointed out by Larson (1974b), if the ISM is sufficiently dense, radiative cooling of supernova remnants (SNRs) can reduce the efficiency of supernova heating by an order of magnitude. The condition for supernova heating to be 100 per cent efficient is that SNRs intersect before radiative cooling becomes important. The time-scale for intersection of SNRs is

$$t_{\rm int} = 8 \times 10^4 E_{50}^{-3/11} \rho_{25}^{3/11} \rho_{*,20}^{-5/11} R_{54}^{-5/11} \,{\rm yr}\,, \tag{34}$$

where E_{50} is the kinetic energy of the supernova ejecta in units of 10^{50} erg, ρ_{25} is the ISM density in units of $10^{-25}\,{\rm g\,cm^{-3}}$, $\rho_{*,20}$ is the stellar density in units of $10^{-20}\,{\rm g\,cm^{-3}}$ and R_{54} is the number of supernovae per second per 10^{54} grammes of stars.

The time-scale for onset of radiative cooling is

$$t_{\rm cool} = 10^5 E_{50}^{16/73} \rho_{25}^{-41/73} \,{\rm yr}\,. \tag{35}$$

These equations have been derived using the similarity solution for the adiabatic blast wave (Taylor 1950) and the approximate cooling law equation (23). Taking the values used for the numerical calculations, $E_{50} = 4$ and $R_{54} = 1$, we have

$$t_{\rm int}/t_{\rm cool} = 0.41\, \rho_{25}^{670/803} \rho_{*,20}^{-5/11}\,. \tag{36}$$

At the centres of sequences DA and KA, we find $t_{\rm int}/t_{\rm cool} = 0.01$ and 0.07 respectively. For the bulk of the galaxy we also find $t_{\rm int}/t_{\rm cool} = 0.07$ in both cases. However, before we can conclude that radiative cooling of the SNRs is negligible for the total outflow models, we have also to check that the ISM pressure does not confine the SNRs and prevent them intersecting. The condition for this is that the ram pressure of the post shock material be greater than the pressure of the ISM. This is true for times less than

$$t_{\rm conf} = 2.5 \times 10^4 \rho_{25}^{-1/3} T_7^{-5/6} \,{\rm yr}\,, \tag{37}$$

where T_7 is the temperature of the ISM in units of 10^7K. For the centres of sequences DA and KA $t_{\rm int}/t_{\rm conf} = 0.07$ and 0.7 respectively. However for the bulk of the galaxy $t_{\rm int}/t_{\rm conf} \simeq 2$. Hence the possibility may arise that the efficiency of supernova heating is significantly reduced in the outer part of the galaxy, making inflow more likely than our models indicate. It seems likely that non-intersection of SNRs will result in a multiphase ISM, rather than our assumed single-component model. The effects of two or more phases to the ISM in elliptical galaxies is an important problem that requires investigation.

In the early epoch models, the high gas density of the inflowing material also results in reduction of the supernova heating efficiency due to radiative cooling of the SNRs. Furthermore pressure confinement of the SNRs occurs in the region of outflow. The reduction in efficiency of supernova-heating will lead to a greater region of inflow than the numerical models suggest.

Thermal conduction by electrons has also been neglected. If there is no magnetic field component perpendicular to the temperature gradient, the equations of Bregman (1978) can be used to calculate the conductive flux. We find that the conductive luminosity is roughly 20 per cent of the supernova heating rate for sequences DA and KA and hence is not completely negligible. However, comparison of electron mean free path and radius of gyration shows that magnetic fields of less than 10^{-17}G are sufficient to suppress electron conduction. Conduction can also be ignored in the partial winds because the low temperatures encountered in the cold inflowing regions result in a greatly reduced conduction coefficient.

Although galaxies undoubtedly have haloes of dark matter (Faber & Gallagher 1979), for simplicity we have not included one in our galaxy models. A measure of the importance of a halo in retarding an outflow by binding gas to the galaxy is the ratio between the central potentials of the dark and luminous components of the galaxy. This quantity is uncertain but the results of Einasto, Kaasik & Saar (1974) for ellipticals indicate that it is probably less than unity, and hence our results are not significantly altered by the existence of haloes.

We have shown that the conditions required for the occurrence of inflow are quite readily met in many galaxies. However, before we can discuss the relevance of our models to nuclear activity we have to check that galaxies moving through the intergalactic medium (IGM) can retain their inflowing gas and are not stripped by the ram-pressure of their motion. Numerical models of ram-pressure stripping for spherical galaxies have been computed by Gisler (1976) and Lea & De Young (1976). Using an analytic approximation derived by Gisler (1976) from his numerical results, we find that ram-pressure stripping will be effective in sweeping interstellar gas out of an elliptical galaxy if

$$\rho_{\rm IGM}\, V_{\rm G}^2 \gtrsim \frac{M_{\rm T}}{r_{\rm e}^3}\,\frac{GM_{\rm T}}{r_{\rm e}}\left(\frac{r_{\rm e}^3}{GM_{\rm T}}\right)^{1/2}\alpha\,. \tag{38}$$

Here $\rho_{\rm IGM}$ is the density of the IGM and $V_{\rm G}$ is the velocity of the galaxy relative to the IGM. We see immediately that ram-pressure stripping is less effective at early epochs when α is larger than at present. As a galaxy with inflowing stellar mass loss evolves it will at some stage begin to lose its ISM either because of ram-pressure stripping or due to supernova-heating. We see from the inequalities (18) and (38) that ram-pressure stripping will be the initial cause of gas loss if

$$\frac{n_{\rm e}}{10^{-3}\,{\rm cm^{-3}}}\left(\frac{V_{\rm G}}{1000\,{\rm km\,s^{-1}}}\right)^2 \gtrsim 15\left(\frac{\alpha_{\rm SN}\,E_{\rm SN}}{4\times10^{-4}\,{\rm erg\,s^{-1}}}\right)\left(\frac{M_{\rm T}}{10^{11}M_\odot}\right)^{1/2}\left(\frac{r_{\rm e}}{1\ {\rm kpc}}\right)^{-3/2}. \tag{39}$$

Here σ^2 has been expressed in terms of $M_{\rm T}$ and $r_{\rm e}$ by the relation for de Vaucouleurs galaxies (*cf.* Bailey & MacDonald 1981a). Further progress can be made if ellipticals are essentially a

one-parameter family, e.g. if we assume ellipticals have a constant mass-to-light ratio, the '$L-\sigma^4$', law relating luminosity to observed velocity dispersion (Terlevich *et al.* 1981 and references therein) can be used to derive a relation between r_e and M_T. For mass-to-light ratios typical of ellipticals (about 30 if $H_0 = 100\,\mathrm{km\,s^{-1}\,Mpc^{-1}}$, Tonry 1980) we find

$$\frac{r_e}{1\ \mathrm{kpc}} \simeq \left(\frac{M_T}{10^{11} M_\odot}\right)^{1/2} h^{-1/2}, \tag{40}$$

where h is Hubble's constant H_0 in units of $100\,\mathrm{km\,s^{-1}\,Mpc^{-1}}$. Equation (59) then becomes, when allowance is made for the dependence of α_{SN} on h,

$$\frac{n_e}{10^{-3}\,\mathrm{cm^{-3}}} \left(\frac{V_G}{1000\,\mathrm{km\,s^{-1}}}\right)^2 \gtrsim 20 \left(\frac{M_T}{10^{11} M_\odot}\right)^{-1/4} h^{11/4}. \tag{41}$$

Hence ram-pressure stripping is of greater importance than supernova heating for the more massive ellipticals. Conditions most conducive to efficient sweeping are found at the centres of the X-ray emitting clusters. For the centre of the Coma cluster $n_e \simeq 2 \times 10^{-3} h^{-1}\,\mathrm{cm^{-3}}$ (Bahcall & Sarazin 1977; Strimpel & Binney 1979) and $V_G \simeq 1800\,\mathrm{km\,s^{-1}}$ (Rood *et al.* 1972). We see from equation (41) that ram-pressure sweeping need be considered only in galaxies with masses $\gtrsim 10^{13} h^{15} M_\odot$. The strong dependence on h makes it difficult to make any hard and fast conclusions until H_0 is better determined. However, there is statistical evidence (Gisler 1978) that sweeping is an important factor in driving gas out of all types of galaxies, not just ellipticals, at the centres of the great clusters. Away from the cluster centre both the IGM density and the velocity dispersion are lower. For example, the ram-pressure drops to about 0.1 of its central value at $\simeq 3$ cluster core radii, the exact position depending on the run of temperature in the X-ray emitting gas. Since over 80 per cent of the cluster galaxies are outside 3 core radii, we see from equation (61) that ram-pressure stripping is ineffective compared with supernova heating at all epochs for the majority of cluster ellipticals for any plausible value of H_0. Furthermore, since the dynamical time-scale for the cluster is $\sim 10^9$ yr, significant amounts of gas can build up even in those outlying galaxies that occasionally pass through the centre (Rood *et al.* 1972 argue against the majority of outlying galaxies having primarily radial motions). Lea & De Young (1976) suggest that it is these galaxies that give tail radio sources.

6 Discussion and implications for nuclear activity

We have shown that at early epochs supernova-heating is incapable of driving a total wind in elliptical galaxies. Instead matter lost from stars flows inwards in sufficient quantities to fuel even the most energetic radio sources. We have not included any sinks such as a central massive black hole in our models and hence *steady state* solutions with an inflowing region do not exist. However the analytic results of Section 4 indicate that transition from inflow to total outflow does not occur earlier than a time

$$t_{tr} \sim 10^9 \left(\frac{\bar{\sigma}}{100\,\mathrm{km\,s^{-1}}}\right)^2 \mathrm{yr}, \tag{42}$$

where $\bar{\sigma}$ is the line-of-sight velocity dispersion averaged over the whole galaxy. Hence inflow is expected to be occurring at the present epoch in elliptical galaxies with $\bar{\sigma} \gtrsim 300\,\mathrm{km\,s^{-1}}$. This conclusion is in full agreement with the results of the numerical calculations.

There is also observational evidence to support the idea that there is a critical velocity dispersion above which stellar mass loss flows inwards and fuels nuclear activity in elliptical

galaxies. Of the 15 ellipticals with central velocity dispersion known to be greater than 275 km s^{-1} (Schechter 1980; Terlevich *et al.* 1981 and references therein), 12 are radio sources (Heeschen 1970; Ekers & Ekers 1973; Dressel & Condon 1978). The remaining three galaxies are NGC 1573, NGC 1600 and NGC 4889. As far as the authors know, NGC 1573 has not been observed at radio wavelengths. NGC 1600 is in the survey of Ekers & Ekers (1973) but was not detected and NGC 4889, a cD galaxy, is the brightest member of the X-ray emitting Coma cluster. It has been suggested (Valtonen & Byrd 1979) that NGC 4889 is orbiting its less bright, but possibly more massive companion cD galaxy, NGC 4874 at a velocity ~ 1800 km s^{-1} (if $H_0 = 100$ km s^{-1} Mpc^{-1}).

Also recent X-ray observations indicate that the hot gas is centred on NGC 4874 and is probably moving with it. It therefore seems likely that NGC 4889 is an example of a ram-pressure stripped galaxy. Thermal conduction from the hot intergalactic gas may also be playing a role in driving gas out of NGC 4889 (Cowie & Songaila 1977). It is also interesting to note that in none of the five high velocity dispersion radio sources that have been observed at 21 cm, was a definite neutral hydrogen content found.

Of the 38 galaxies with σ known to be less than 275 km s^{-1}, only five are radio sources. Furthermore four of these five galaxies, NGC 1052 (Knapp, Gallagher & Faber 1978; Reif, Mebold & Goss 1978; Fosbury *et al.* 1978), NGC 4278 (Bottinelli & Gouguenheim 1977a; Gallagher *et al.* 1977; Bieging 1978), NGC 4636 (Bottinelli & Gouguenheim 1977b; Knapp, Faber & Gallagher 1978; Knapp, Kerr & Henderson 1979) and NGC 5846 (Huchtmeier, Tammann & Wendker 1977; Bottinelli & Gouguenheim 1979) contain detectable amounts of neutral hydrogen. The fifth galaxy, NGC 7785, has not been observed at 21 cm.

The presence of H I in those active galaxies with $\sigma < 275$ km s^{-1} and the lack of it in active galaxies with $\sigma > 275$ km s^{-1} suggests that the radio emission has a different cause in each case.

Gunn (1979) has outlined a model for the cause of the activity in NGC 1052 and 4278 in which the neutral hydrogen has come into the galaxy from outside. Further evidence for this external origin of the gas comes from the large difference (~ 70°) between the direction of the axis of the neutral hydrogen disc and the rotation axis of the stars in NGC 4278 (Gunn 1979). The exact source of the neutral gas has become uncertain because the original proposal of Gunn that it is infall of intergalactic H I clouds has been ruled out by recent observations (Lo & Sargent 1979; Haynes & Roberts 1979).

It is our contention that inflowing stellar mass loss fuels nuclear activity in elliptical galaxies with $\sigma \gtrsim 275$ km s^{-1}. If the elliptical galaxy has a well-defined stellar rotation axis, the stellar mass loss should also rotate around this axis and hence rotation axes determined from absorption lines and emission lines should be parallel. This has been shown to be the case by Simkin (1979).

Slowly moving, massive galaxies such as M87, at the centres of clusters may also be fuelled by radiative accretion of gas lost from the cluster galaxies (Mathews & Bregman 1978).

The dependence of $t_{\rm tr}$ on $\bar{\sigma}$ has an important consequence for the density evolution of radio sources. The correlation between $\bar{\sigma}$ and B magnitude, $M_{\rm B}$, for elliptical galaxies (Terlevich *et al.* 1981) leads to

$$\frac{t_{\rm tr}}{10^{10}\,{\rm yr}} \simeq 0.5\,h^{-1}\,10^{-0.192\,(M_{\rm B}+21.0)}. \tag{43}$$

Hence at the present epoch only galaxies with $M_{\rm B} \leqslant M_{\rm B,act} \simeq -21$ may be active. This conclusion can be altered either by infall of gas from outside (see above) or if gas has been left over from a previous period of activity (Bailey 1980). Our limit is brighter than the characteristic magnitude ($M_{\rm B}^{*} = 19.8$ for $H_0 = 85$ km s^{-1} Mpc^{-1}, Kirshner, Oemler & Schechter 1979)

in the galaxy luminosity function of Schechter (1976) and hence a small evolutionary decrease in $M_{B,act}$ will lead to a large decrease in the comoving number density of active galaxies. The evolution of the radio source density function is discussed in greater depth in Bailey & MacDonald (1981b).

The cause and form of nuclear activity is intimately connected with the fate of the inflowing gas. In the numerical models the net angular momentum of the stars was neglected. Since elliptical galaxies are, in general, slow rotators (Illingworth 1977; Peterson 1978; Davies 1981) this is justifiable in the case of total outflow. However, because of the large stagnation radii encountered, angular momentum cannot be neglected when inflow occurs. For example, the observations by Davies (1981) give a rotation velocity of $\sim 50\,\mathrm{km\,s^{-1}}$ for NGC 3379 at about 20 arcsec (~ 700 pc) from the centre. In sequences KC and DC stagnation radii greater than this are attained. If gas flows inwards from this region, conserving its angular momentum, the centrifugal force is comparable with gravity when the gas is ~ 100 pc from the centre. Hence a disc of cold gas of dimension ~ 100 pc is expected to form. The detailed structure and evolution of this disc will depend on the degree of dissipation in the disc, on the structure and rotation law of the galaxy and also on whether or not the cooling, inflowing material breaks up into clouds due to Rayleigh–Taylor instability. If the flow remains smooth (as it does in the King models), infalling gas mixes with freshly injected material of lower specific angular momentum and hence centrifugal forces will be lower, and the disc smaller, than for the case in which the inflow breaks up (as it probably does in the de Vaucouleurs models) into small dense clouds which have little interaction with newly injected gas. This again highlights the importance of studies dealing with the multiphase flows.

Under the assumption that material arrives at the disc in centrifugal equilibrium, Bailey (1980) has shown that a self-gravitating object of mass $\sim 10^3 M_\odot$ and radius ~ 3 pc forms in the nucleus of the elliptical galaxy when the disc mass $\sim 10^6 M_\odot$. The subsequent evolution depends critically on whether further fragmentation occurs, leading to ordinary star formation or whether the original self-gravitating object collapses as a whole to form a supermassive star, low-mass spinar or black hole.

Since, in our model, the fraction of ellipticals with inflowing stellar mass loss decreases with time, if star formation occurs, the ratio of blue to red elliptical galaxies in clusters should increase with cluster redshift. Such an effect has been observed by Butcher & Oemler (1978) who found that two distant ($Z \simeq 0.4$) clusters have roughly equal numbers of blue and red galaxies whereas the nearby Coma cluster, of comparable richness and central condensation to the distant clusters, consists entirely of ellipticals and SOs.

If there is a black hole at the Galactic Centre, inflowing stellar mass loss can be converted into energy at prodigious rates. Lynden-Bell (1978) has shown that efficiencies of 1/3 are easily attained from disc accretion on to a rotating black hole. At this efficiency, an accretion rate, $FM_\odot\,\mathrm{yr}^{-1}$, produces an accretion luminosity

$$L_{acc} = 4 \times 10^{12} F L_\odot . \tag{44}$$

The Eddington limiting luminosity for a black hole of mass M_{BH} is

$$L_{Ed} = 3 \times 10^4 \frac{M_{BH}}{M_\odot} L_\odot . \tag{45}$$

Hence accretion is supercritical if

$$M_{BH} \lesssim 10^8 F M_\odot . \tag{46}$$

F is a decreasing function of time whilst M_{BH} increases with time. Hence accretion, which may be supercritical at early epochs, later becomes subcritical and eventually ceases when

total outflow begins. The supercritical phase can be associated with quasars and the formation of double-lobe radio sources (Lynden-Bell 1978). During the subcritical phase the galaxy will still have a bright optical core (N galaxy?) which will fade with time and disappear completely when the fuel supply to the black hole is finally turned off.

7 Conclusions

Our main conclusions can be summarized as follows:

(1) Supernova heating cannot prevent stellar mass loss flowing inwards for a large proportion of the lifetime of giant elliptical galaxies, irrespective of the detailed structure of the underlying galaxy.

(2) Secular evolution of the mass loss rate produces a rapid increase in the comoving density of active galaxies, as observed.

(3) Our model gives a natural explanation for the association of nuclear activity with galaxies of higher velocity dispersion and luminosity.

Acknowledgments

We thank Clinton Blackman, Philip Hughes, John Lucey and Bill Pence for interesting and helpful discussions, Professor Roger Tayler for a critical reading of the manuscript and the referee for suggesting improvements to the presentation. This work is supported by the SRC.

References

Allen, C. W., 1973. *Astrophysical Quantities,* 3rd edn, Athlone Press, London.
Bahcall, J. B. & Sarazin, C. L., 1977. *Astrophys. J.,* **213,** L99.
Bailey, M. E., 1980. *Mon. Not. R. astr. Soc.,* **191,** 195.
Bailey, M. E. & MacDonald, J., 1981a. *Mon. Not. R. astr. Soc.,* **194,** 195.
Bailey, M. E. & MacDonald, J., 1981b. *Nature,* **289,** 659.
Beiging, J. H., 1978. *Astr. Astrophys.,* **64,** 23.
Bottinelli, L. & Gouguenheim, L., 1977a. *Astr. Astrophys.,* **54,** 641.
Bottinelli, L. & Gouguenheim, L., 1977b. *Astr. Astrophys.,* **60,** L23.
Bottinelli, L. & Gouguenheim, L., 1979. *Astr. Astrophys.,* **74,** 172.
Bregman, J. N., 1978. *Astrophys. J.,* **224,** 768.
Burke, J. R. & Silk, J., 1974. *Astrophys. J.,* **190,** 1.
Butcher, H. & Oemler, A., 1978. *Astrophys. J.,* **219,** 18.
Cameron, A. G. W., 1973. In *Explosive Nucleosynthesis,* ed. Schramm, D. N. & Arnett, W. D., University of Texas Press, Austin.
Coleman, G. D. & Worden, S. P., 1976. *Astrophys. J.,* **205,** 475.
Coleman, G. D. & Worden, S. P., 1977. *Astrophys. J.,* **218,** 792.
Colla, G., Fanti, C., Fanti, R., Gioia, I., Lari, C., Lequeux, J., Lucas, R. & Ulrich, M-H., 1975. *Astr. Astrophys.,* **38,** 209.
Condon, J. J. & Dressel, L. L., 1978. *Astrophys. J.,* **221,** 456.
Cowie, L. L. & Songaila, A., 1977. *Nature,* **266,** 501.
Davies, R. L., 1981. *Mon. Not. R. astr. Soc.,* **194,** 879.
de Vaucouleurs, G., 1959. *Handb. Phys.,* **53,** 311.
de Vaucouleurs, G. & Capaccioli, M., 1979. *Astrophys. J. Suppl.,* **40,** 699.
De Young, D. S., 1976. *A. Rev. Astr. Astrophys.,* **14,** 447.
Dressel, L. L. & Condon, J. J., 1978. *Astrophys. J. Suppl.,* **36,** 53.
Einasto, J., Kaasik, A. & Saar, E., 1974. *Nature,* **250,** 309; Erratum, *Nature,* **250,** 790.
Ekers, R. D. & Ekers, J. A., 1973. *Astr. Astrophys.,* **24,** 247.
Faber, S. M. & Gallagher, J. S., 1976. *Astrophys. J.,* **204,** 365.
Faber, S. M. & Gallagher, J. S., 1979. *A. Rev. Astr. Astrophys.,* **17,** 135.

Fosbury, R. A. E., Mebold, U., Goss, W. M. & Dopita, M. A., 1978. *Mon. Not. R. astr. Soc.*, **183,** 549.
Gallagher, J. S., Knapp, G. R., Faber, S. M. & Balick, B., 1977. *Astrophys. J.*, **215**, 463.
Gisler, G. R., 1976. *Astr. Astrophys.*, **51,** 137.
Gisler, G. R., 1978. *Mon. Not. R. astr. Soc.*, **183,** 633.
Gorenstein, P. & Tucker, W. H., 1976. *A. Rev. Astr. Astrophys.*, **14,** 373.
Gunn, J. E., 1979. In *Active Galactic Nuclei,* eds Hazard, C. & Mitton, S., Cambridge University Press.
Haynes, R. P. & Roberts, M. S., 1979. *Astrophys. J.*, **227,** 767.
Heeschen, D. S., 1970. *Astrophys. Lett.*, **6,** 49.
Henyey, L. G., Wilets, L., Böhm, K. H., Lelevier, R. & Levee, R. D., 1959. *Astrophys. J.*, **129,** 628.
Huchtmeier, W. K., Tammann, G. A. & Wendker, H. J., 1977. *Astr. Astrophys.*, **57,** 313.
Illingworth, G., 1977. *Astrophys. J.*, **218,** L43.
Joy, A. H. & Abt, H. A., 1974. *Astrophys. J. Suppl.*, **28,** 1.
Kafatos, M., 1973. *Astrophys. J.*, **182,** 433.
King, I. R., 1966. *Astr. J.*, **71,** 64.
King, I. R., 1978. *Astrophys. J.*, **222,** 1.
Kirshner, R. P., Oemler, A. & Schechter, P. L., 1979. *Astr. J.*, **84,** 951.
Knapp, G. R., Faber, S. M. & Gallagher, J. S., 1978. *Astr. J.*, **83,** 11.
Knapp, G. R., Gallagher, J. S. & Faber, S. M., 1978. *Astr. J.*, **83,** 139.
Knapp, G. R., Kerr, F. J. & Henderson, A. P., 1979. *Astrophys. J.*, **234,** 448.
Kunkel, W. E., 1973. *Astrophys. J Suppl.*, **25,** 1.
Kunkel, W. E., 1975. In *IAU Symp. 67: Variable Stars and Stellar Evolution,* eds Sherwood, V. E. & Plaut, L., Reidel, Dordrecht.
Larson, R. B., 1974a. *Mon. Not. R. astr. Soc.*, **166,** 585.
Larson, R. B., 1974b. *Mon. Not. R. astr. Soc.*, **169,** 229.
Lo, K. Y. & Sargent, W. L. W., 1979. *Astrophys. J.*, **227,** 756.
Lea, S. M. & De Young, D. S., 1976. *Astrophys. J.*, **210,** 647.
Lynden-Bell, D., 1978. *Phys. Scripta,* **17,** 185.
Malin, D. F. & Carter, D., 1980. *Nature,* **285,** 643.
Mathews, W. G. & Baker, J. C., 1971. *Astrophys. J.*, **170,** 241.
Mathews, W. G. & Bregman, J. N., 1978. *Astrophys. J.*, **224,** 308.
Minkowski, R. & Osterbrock, D., 1959. *Astrophys. J.*, **129,** 583.
Oemler, A. & Tinsley, B. M., 1979. *Astr. J.*, **84,** 985.
Osterbrock, D. E., 1960. *Astrophys. J.*, **132,** 325.
Peterson, C. J., 1978. *Astrophys. J.*, **222,** 84.
Raymond, J. C., Cox, D. P. & Smith, B. W., 1976. *Astrophys. J.*, **204,** 290.
Reif, K., Mebold, U. & Goss, W. M., 1978. *Astr. Astrophys.*, **67,** L1.
Rood, H. J., Page, T. L., Kintner, E. C. & King, I. R., 1972. *Astrophys. J.*, **175,** 627.
Salpeter, E. E., 1955. *Astrophys. J.*, **121,** 161.
Sargent, W. L. W., Young, P. J., Boksenberg, A., Shortridge, K., Lynds, C. R. & Hartwick, F. D. A., 1978. *Astrophys. J.*, **221,** 731.
Schechter, P., 1976. *Astrophys. J.*, **203,** 297.
Schechter, P. L., 1980. *Astr. J.*, **85,** 801.
Schweizer, F., 1979. *Astrophys. J.*, **233,** 23.
Searle, L., 1974. *Astrophys. Space Sci.*, **45,** 125.
Shapiro, P. R. & Moore, R. T., 1976. *Astrophys. J.*, **207,** 460.
Shklovskii, I. S., 1978. *Soviet Astr.*, **22,** 413.
Simkin, S. M., 1979. *Astrophys. J.*, **234,** 56.
Strimpel, O. & Binney, J., 1979. *Mon. Not. R. astr. Soc.*, **188,** 883.
Tammann, G. A., 1974. *Astrophys. Space Sci.*, **45,** 155.
Tammann, G. A., 1977. *Astrophys. Space Sci.*, **66,** 95.
Taylor, G., 1950. *Proc. R. Soc.*, **A201,** 159.
Terlevich, R., Davies, R. L., Faber, S. M. & Burstein, D., 1981. *Mon. Not. R. astr. Soc.*, **196,** 381.
Tinsley, B. M., 1976. *Astrophys. J.*, **208,** 797.
Tinsley, B. M., 1977. *Astrophys. Space Sci.*, **66,** 117.
Tonry, J. L., 1980. *PhD Thesis,* Harvard University.
Valtonen, M. J. & Byrd, G. G., 1979. *Astrophys. J.*, **230,** 655.
Wheeler, J. C. & Hansen, C. J., 1971. *Astrophys. Space Sci.*, **11,** 373.
Whelan, J. & Iben, I., 1973. *Astrophys. J.*, **186,** 1007.